SEISMIC BEHAVIOR OF PREFABRICATED COLUMN-FOOTING CONNECTION

A. A. Tasnimi

Department of Civil Engineering, School of Engineering
Tarbiat Modarres University
Tehran, Iran

(Received: July 20, 1998 - Accepted in Revised Form: April 8, 1999)

Abstract Results of an experimental investigation of the seismic performance of prefabricated column-footing connections are presented. Tests were conducted on six 1/4-scale prefabricated column specimens inserted into prefabricated footings in two groups. Group-1 consisted of four specimens, which were tested under constant axial load and cyclic inelastic lateral displacements. The remaining two specimens in group-2, were subjected to cyclic inelastic lateral displacements only for comparison. Test results showed that this type of connection exhibits relatively higher ultimate strength comparable to fixed end connections, and fairly acceptable ductile behavior. Also the test results indicate the strength reduction in post-elastic state and the connection behavior as a semi-rigid joint.

Key Words Prefabricated, Ductility, Cracking, Lateral Load, Earthquake, Connection, Energy Dissipation

چکیده در این مقاله نتایج به دست آمده از بررسی آزمایشگاهی رفتار لرزه‌ای اتصال ستون به شالوده گلدانی در سازه‌های بتن مسلح پیش‌ساخته ارایه شده است. بدین منظور اتصال مزبور که مورد استفاده در ساختمان‌های پیش‌ساخته صنعتی است، انتخاب و ۶ نمونه در مقیاس ۱/۴ و در دو گروه مدل شده و مورد مطالعه قرارگرفت. در گروه اول ۴ نمونه تحت اثر نیروی محوری ثابت و نیروی جانبی رفت و برگشتی و در گروه دوم ۲ نمونه تحت اثر نیروی جانبی رفت و برگشتی مورد آزمایش قرارگرفتند. نیروی جانبی رفت و برگشتی تا مراحل غیرارتجاعی به هر دو گروه اعمال گردید. رفتار هر یک از اجزای اتصال، همچنین مقاومت و شکل‌پذیری اتصال موردمطالعه واقع شد. نتایج حاصله نشان می‌دهد که این گونه اتصالات در مقابل نیروهای وارده مقاومت کافی داشته ولی به دلیل نحوهٔ اجرای اتصال استهلاک انرژی در آنها متوسط می‌باشد. هرچند سهولت اجراء، صرفه‌جویی اقتصادی و امکان تهیه با کیفیت بالا نیز از محاسن دیگر این اتصالات به شمار می‌رود؛ اما باید به نحوی ظرفیت جذب انرژی افزایش داده شود.

INTRODUCTION

There is a lack of investigation on the seismic behavior of prefabricated reinforced concrete columns inserted into the prefabricated foundation in precast concrete frames. In general this type of connection is considered as rigid joints. Lateral load caused by earthquake or wind imposes axial and high horizontal forces and bending moments to connections of precast concrete framing systems, which are obliged to resist such forces. This occurs during a large number of inelastic cycles while the joint needs to dissipate large amount of energy. In other words, the column-footing connections must exhibit considerable energy absorption with minimum reduction in strength and stiffness in all states of loading particularly in post-elastic state.

An attempt was made to investigate the behavior of prefabricated column-footing connection and its performance when subjected to cyclic lateral loading. The tested column-footing connections are representatives

of the joints in large span one-bay frames of one-story buildings. Typical beam's span of such frames is 12.0m. The height of columns is 5.0m which has 550×450mm dimension. Such buildings are generally used for factories, offices, warehouses laboratories etc. In this type of construction the prefabricated column is embedded in their prefabricated footing in a special pocket. The connection is made by pouring the concrete grout into the pocket and around the column. This type of connection is generally considered as a rigid joint to resist axial force, shear force, and bending moment induced by gravity and earthquake loads. The analysis was carried out for gravity and earthquake loads recommended by Iranian minimum design load for ordinary buildings and structures (IS519) [1], and Iranian code for seismic resistant design of buildings (IS2800) [2], respectively. The design of the prototype as well as specimens was based on ACI recommendation [3].

A total of six 1/4-scale rectangular prefabricated reinforced concrete columns were cast and connected to prefabricated reinforced concrete footings. The footings were fixed to the laboratory base and the columns were tested under gravity and revered cyclic loading in tow groups. All specimens were identical in size and reinforcement ratio, and the only main variable in these specimens were the applied loads. Group-1 consisted of four specimens which subjected to gravity as well as cyclic lateral loading, where as group-2 specimens were subjected to cyclic lateral load only. Results of the tests conducted are discussed.

RESEARCH SIGNIFICANCE

The purpose of the experimental study described in this paper is to investigate the seismic behavior of prefabricated column-footing connections when subjected to cyclic lateral loading in the elastic and inelastic states.

EXPERIMENTAL PROGRAM

Test Specimens Six rectangular, prefabricated reinforced concrete column footing assemblages were designed with a scale factor 1/4 that of the prototype one-bay and one-story building columns. Dead and live loads were calculated on the basis of IS519 which deals with minimum design load for ordinary buildings and structures [1]. The test specimens were designed on the basis of design recommendations given by Iranian code of practice for seismic resistant design of the buildings [2]. Two groups of specimens are considered in this study. The first group consisted of four specimens, which were tested under constant axial load (gravity) and cyclic lateral loading simultaneously. These specimens were designated by G1LA1, 2, 3, 4. The second group comprised two specimens which were tested under cyclic lateral loading only and designated by G2LO5, 6. The dimensions of the prefabricated reinforced concrete column footings were determined so that the test units fit the laboratory space and equipment limitation. The overall height of the test units was 760mm and that of columns was 970mm.

The footing's height was 287.5mm with 682mm in length and 550mm in width. Depth of the footing's pocket was 210mm in which the lower portions of the columns were inserted. The criterion used in the modeling of specimens is given in reference 9. The casting of the specimens carried out in two sets of concrete batches but at different times, so that three test units were cast at the same time using the first

batch of concrete mix. The remaining test units were also cast at the same time using the second concrete batch. After one week when the components of test units gained 70% of their ultimate strength, columns were inserted into the footings while keeping them precisely in vertical position. Pouring the concrete grout into the footings pocket surrounding the columns made the connection. The test configuration, percentages of reinforcement and the mechanical properties of materials were similar. Typical dimensions, reinforcement and the connection for all specimens are illustrated in Figure. 1.

Materials The choice of the model materials is important in modeling small-scale reinforced concrete members. The specified characteristic strengths of all materials were selected to be similar to that of the prototype structure. The concrete used in all specimens consisted of ordinary portland cement, natural glacial sand, and coarese aggregate with maximum size of 10 mm. The mix design was carried out on the basis of Rood Note no. 4 [4]. This mix resulted in cylinder strength at 28 days tabulated in Table 1. Typical stress-strain curve for concrete used in all specimens is shown in Figure 2. The average compressive strength from the test cylinders at the time of connection testing was 20.5 MPa and 24.2MPa for columns and footings respectively. The average tensile strength from the splitting test cylinders was 1.95 MPa for columns and 2.62MPa for footings. All reinforcements used in the specimens were tested to obtain their direct tensile strength, using the universal-testing

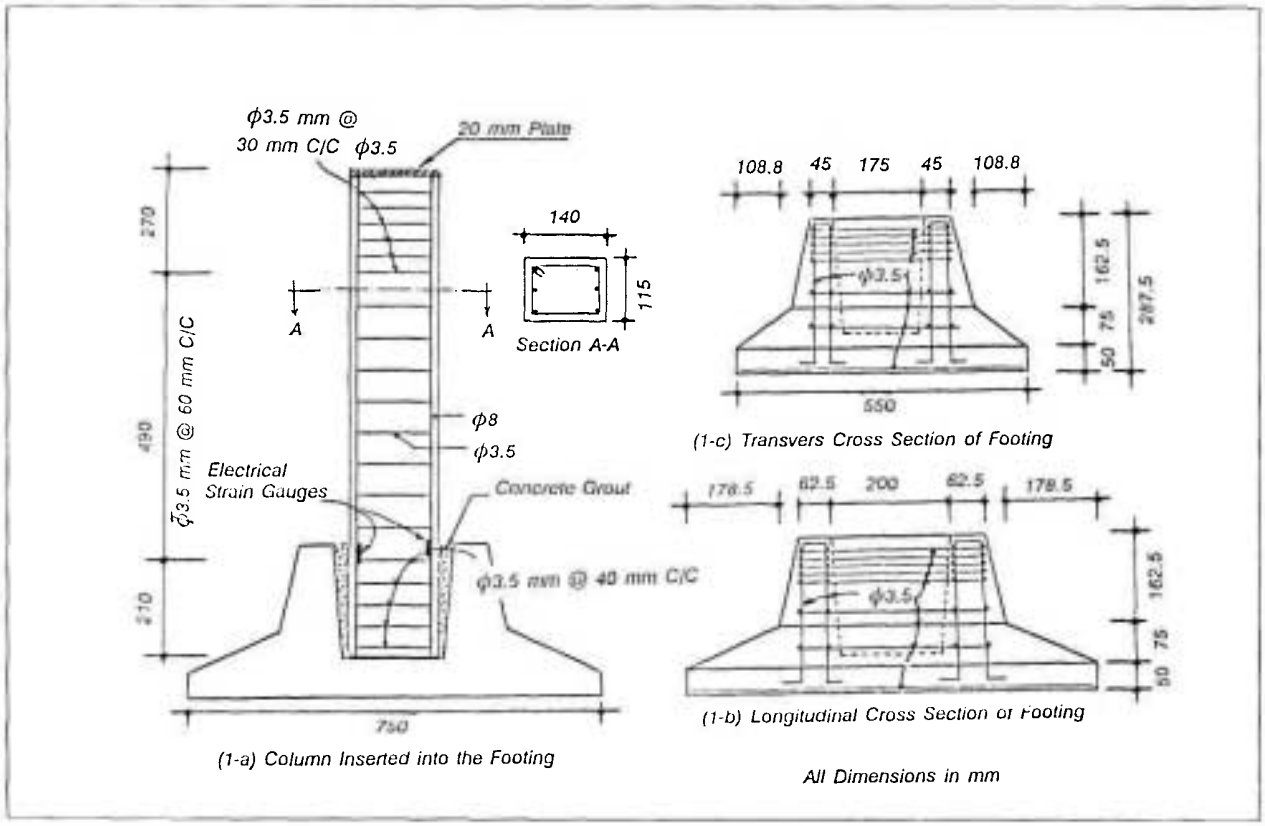

Figure 1. Typical column-footing connection, dimensions and reinforcement

TABLE 1. Measured Concrete Compressive and Tensile Strength.

Sample Number	Samples for Columns		Samples for Footings	
	Tensile Splitting f_{ct} (MPa)	Compressive Cylinder f'_c (MPa)	Tensile Splitting f_{ct} (MPa)	Compressive Cylinder f_c (MPa)
1	2.10	20.1	2.30	24.9
2	1.80	21.3	2.85	23.9
3	1.95	21.3	2.70	23.8
Average	1.95	20.5	2.62	24.2

TABLE 2. Material Properties of steel Reinforcement

Bar Size	Average Yield Stress (MPs)	Average Yield Strain	Average Ultimale Strength(MPa)
ϕ 8	397.6	0.0021	617.3
ϕ 3.5	259.8	0.002	462.5

machine with 450kN capacity. All columns had a 140×115mm rectangular cross section, and were reinforced with 6 No. 8mm diameter longitudinal deformed bars resulting in a reinforcement ratio of 1.87%. The measured yield strength of these bars was 397.6MPa. The transvers reinforcement for all six columns and footings consisted of 3.5 mm diameter mild steel plane bars of measured yield strength of 259.8MPa. These bars were placed at 490mm center portion of columns height at 60mm center to center. The transvers reinforcements were distributed at 30mm c/c at 270mm height of the upper portion of the columns. The same bars were distributed at 40mm c/c at 210mm height of the lower portion of the columns. Table 2 summarizes the material properties of steel reinforcement. Typical stress-strain curves for 8mm and 3.5mm reinforcement used in all specimens are shown in Figure 3.

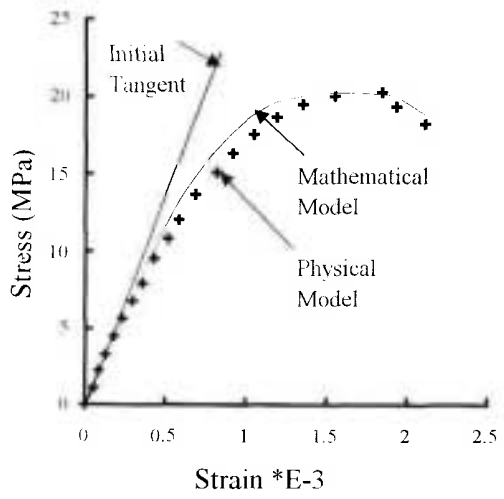

Figure 2. Concrete Stress-Strain Curves.

Test setup The setup was designed for testing column-footing assemblages subjected to lateral loading. The specimens were tested in a steel reaction frame as shown in Figure 4. The

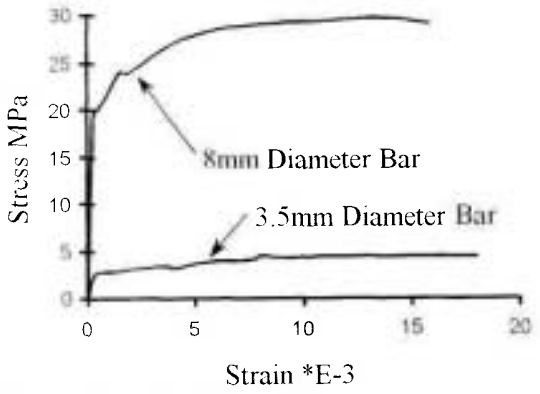

Figure 3. Steel Stress-Strain curves.

prefabricated footings of the test units were fastened through twelve threaded end of 16mm diameter high-strength steel rods against the base beams of the test frame, which was strongly bolted to the laboratory floor. These steel rods were provided underneath of footings before their casting. Two independent loading systems were used to apply the load to the specimens. The axial load of 15.5kN was applied to the first group columns by a one-way hydraulic actuator having 19T capacity. This load was applied to simulate the constant gravity load on the columns. The magnitude of this load was determined based on the scale factor of 1/4 over the roof area resulting in a factor of $1/4 \times 1/4 = 1/16$.

The prototype column load had been designed for a gravity load of kN, resulting in an axial load of 15.5kN on the test columns. The hydraulic actuator of axial load was mounted between two horizontal channel sections (2UP14) of the test frame. A ruling (hinging) system was designed in such a manner that, while the application of lateral load displaces the column head, at the same time causes no eccentricity to the path of axial load. This hinging system consisted of three major portions as, ruling part, column's cap and two chambers for setting two one-way hydraulic

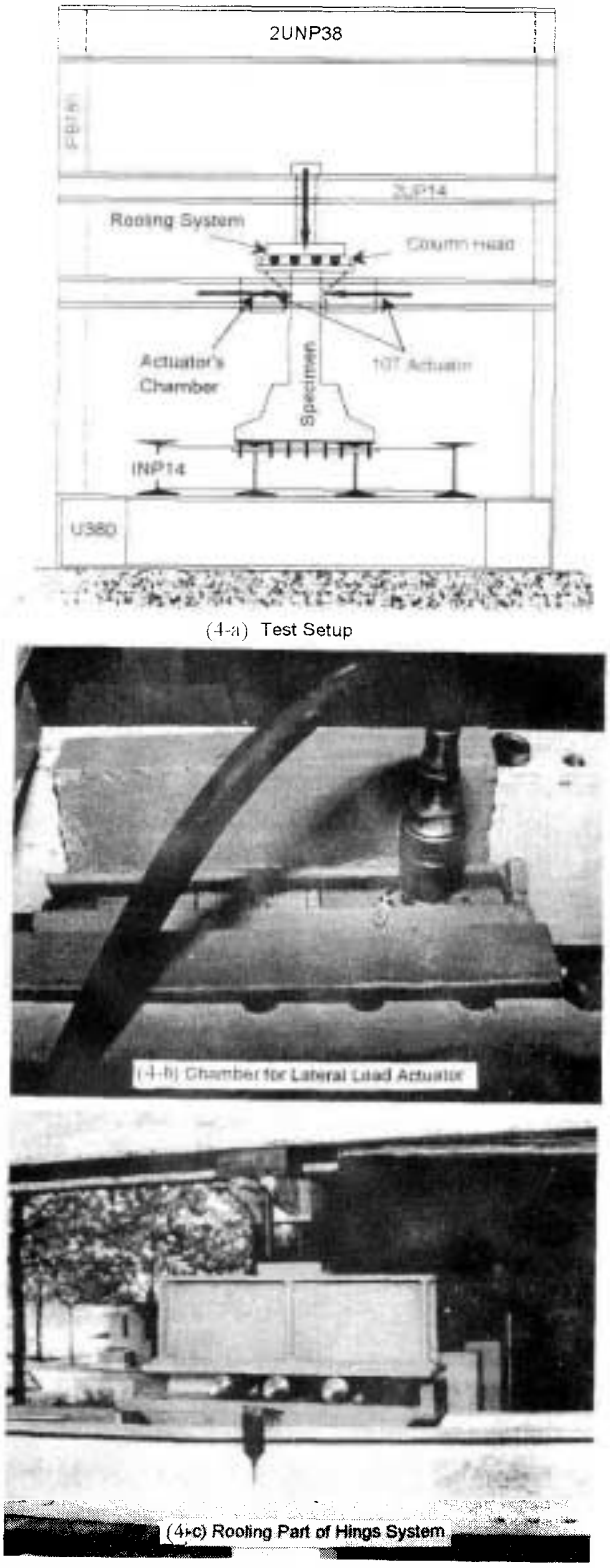

Figure 4. General view of test setup and some details of test arrangement.

actuators by which lateral load had to be applied. These actuators were capable of moving the top of the specimen in both positive and negative directions one after another.

The column's cap was put on the column and then tightened by means of screws. A stiffened INP14 was rested on rollers over the column's cap, allowing lateral moment at the top of the columns during the application of lateral loads. When lateral load was applied from left to right, the right chamber was released and moved back. While the lateral load was applied from right to left, the left chamber was released and moved back. By such an arrangement it was possible to apply lateral load cyclically at top of the column.

Instrumentation Electrical strain gauges of type 6/120-LY41 having 14mm length and 6 mm width were used for strain measurement of vertical reinforcements of pocket portion of precast footing. Also strains of column's longitudinal bars at the vicinity of top of the footing were measured by electrical strain gauges of type 10/120-LY41 with length and width equal to 18 mm and 8 mm respectively. The positions of all strain gauges are shown is Figure l.

KC-20-Al-II type electrical strain gauges were used for surface concrete strains near the joint core, called hereafter as critical section for all specimens. Figure 5-a shows the position of these strain gauges. The displacements of column at various heights were measured using dial gauges with 0.01 mm accuracy attached to the column.

To ensure that the footing is fixed to the framing system, the same dial gauge was used to measure footing displacement if any. Figure 5-b illustrates the position of dial gauges used.

Loading The axial load was kept constant at

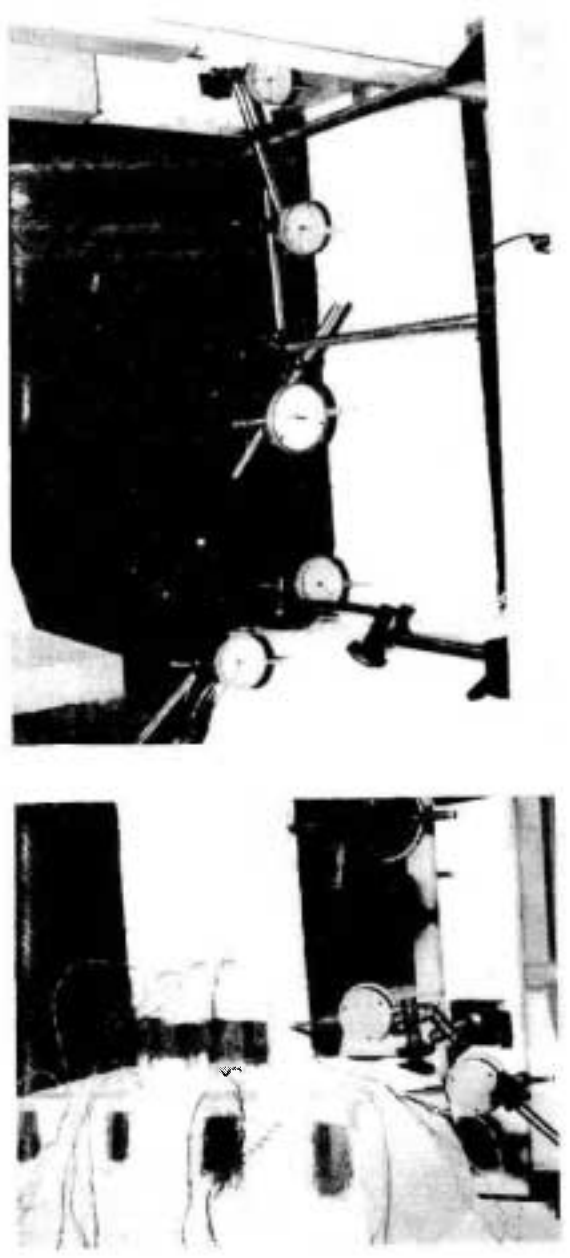

Figure 5. Strain gauges and dial gauges for strain and displacement measurement.

15.5kN during the test. A one-way hydraulic actuator having 10T capacity was used to apply the axial load to the first group of specimens only.

Reversed cyclic loading simulated the effect of an earthquake on column specimen. Two

hydraulic actuators in the test setup were used to displace the top of the column to achieve a pre-determined displacement level. These actuators were used one after another to achive the same displacement level in the opposite direction. This cyclic lateral load was controlled on the basis of displacement ductility ratio, which in turn was evaluated on the basis of a mathematical model of concrete stress-strain relationship [5]. This mathematical model is briefly explained in the following section. The selected load history consisted of two phases. At the first phase, which was related to elastic state, the test was in a load control mode. Upon yielding of the specimen, a displacement control mode of loading was utilized. Figure 6 shows typical loading sequences of the columns. The displacement ductility factor was defined as the ratio of the applied displacement over the displacement at first yielding of the longitudinal bars of the columns.

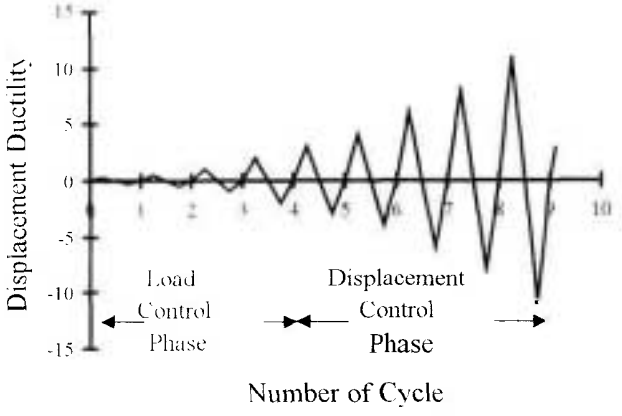

Figure 6. Loading sequence for column's lateral load.

THEORETICAL STUDY

A simplified analytical method was used to predict forces within the section of the specimens. The following assumptions were made in the analysis (1) linear strain distribution through the full depth of the specimens, (2) small deformations, (3) concrete tensile strength at elastic state contributes the equilibrium and (4) elastic-ideally plastic stress-strain relationship for steel reinforcements. Since the horizontal load was applied gradually in successive loading cycles, the strength of all specimens was evaluated analytically at any state of behavior, particularly at yield and ultimate state.

Stress-Strain Curves The mathematical model for the stress-stain relation of concrete given in reference [5] was used to calculate the total compressive and tensile forces, and moment of resistance at any state of loading in the section. The mathematical model in its general form is shown in Figure 8 and given by:

$$\sigma = \alpha\varepsilon^4 + \beta\varepsilon^3 + E_c\varepsilon \quad (1)$$

Where $$\alpha = \left\{\frac{2E_c}{\varepsilon_0^3} - \frac{3f'_c}{\varepsilon_0^4}\right\} \quad (1\text{-a})$$

and $$\beta = \left\{\frac{4f'_c}{\varepsilon_0^3} - \frac{3E_c}{\varepsilon_0^2}\right\} \quad (1\text{-b})$$

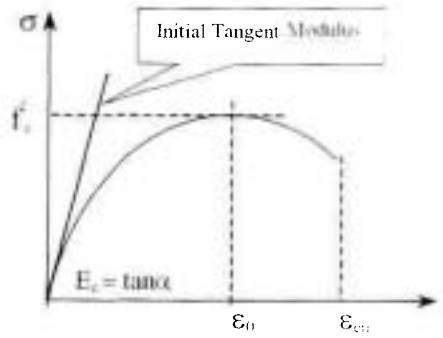

Figure 7. Mathematical Model for concrete stress-strain curves.

Where ε is the value of concrete compressive strain, f'_c is the maximum concrete compressive stress, ε_0 is the concrete strain corresponding to f_c and E_c is the initial tangent modulus of elasticity obtained from concrete cylinder test.

Strength The compressive force at any state of loading, C_i is the sum of the concrete

compressive force, C_{ci} and steel compressive force C_{si} which is given by:

$$C_{ci} = b\int_0^{d_{ni}} \sigma_{xi} d_{xi} \quad (2)$$

$$C_{si} = A_s f'_s = A_s E_s \varepsilon'_s \leq A_s f_y \quad (3)$$

Where σ_{xi} is the concrete compressive stress and d_{ni} is the depth of neutral axis at the i^{th} state of loading. Further, b represents the section width, ε_{xi} is the concrete strain at depth equal to $(d_{ni}-x_i)$ and A'_s, f'_s and ε'_s are the area, stress and strain of the reinforcement at compression side respectively. Figure 8 gives the typical stress, strain distribution and the internal forces across depth of rectangular section.

It is assumed that the strain is distributed linearly across the section. Knowing the extreme concrete compressive strain (ε_{ci}) and assuming a good bonding condition between concrete and reinforcement, the concrete compressive force and steel compressive force could be written in terms of (ε_{ci}).

$$C_{ci} = \frac{b\, d_{ni}}{\varepsilon_{ci}} \int_0^{\varepsilon_{ni}} \sigma_{xi} d\varepsilon_{xi} \quad (4)$$

$$C_{si} = A'_s E_s \varepsilon_{ci} \left(1 - \frac{d'}{d_{ni}}\right) \quad (5)$$

It has been reported that the difference between the concrete limiting tensile strain obtained from splitting tensile test and the value calculated from mathematical model is negligible (about 0.003 percent difference) [5].

The concrete cracking strain or the limiting tensile strain is represented by ε_{ct}. Hence the concrete limiting tensile strain (corresponded to its splitting tensile stress) on the basis of the linear stress-strain relationship was used to evaluate the concrete tensile force whose value is given by:

$$T_{ci} = \frac{1}{2} b\, d_{ni} \frac{E_c \varepsilon_{ct}^2}{\varepsilon_{ci}} \quad (6)$$

The tensile steel strength at tension side is calculated by equation 7:

$$T_{si} = A_s E_s \varepsilon_s \leq A_s f_y \quad (7)$$

Or in terms of concrete strain it is:

$$T_{si} = A_s E_s \varepsilon_{ci} \left(\frac{d}{d_{ni}} - 1\right) \quad (8)$$

Where A_s and f_s are the area and tensile stress of the reinforcement in tension side, the total tensile force of the section would be:

$$T_i = T_{si} + T_{ci} \quad (9)$$

The value of d_{ni} could be evaluated either from the strain distribution across the section obtained from the measured strain in the section, or by equating the total tensile and compressive forces in the section. The equation of equilibrium and the moment of resistance of the section about the neutral axis are given by:

$$N_i = C_{ci} + C_{si} - T_{si} + T_{ci} \quad (10)$$

$$M_i = C_{ci}\left(d_{ni} - d_c\right) + C_{si}\left(d_{ni} - d\right) + \frac{2}{3} T_{si} \frac{d_{ni}\varepsilon_{ct}}{\varepsilon_{ci}} + T_{ci}\left(d - d_{ni}\right) \quad (11)$$

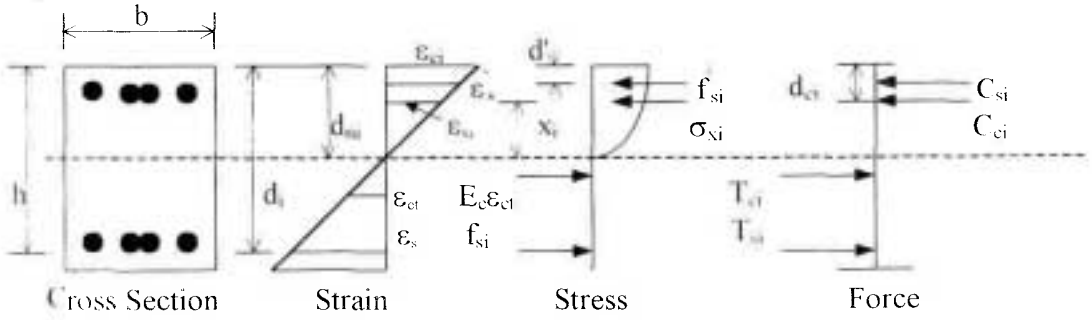

Figure 8. Strain, Stress and force diagrams across depth of rectangular section.

The only unknown in these equations is d_c, which would be obtained by:

$$d_c = d_{ni}\left[1 - \frac{\int_0^{\varepsilon_{ci}} \varepsilon_{xi}\,\sigma_{xi}\,d\varepsilon_{xi}}{\varepsilon_{ci}\int_0^{\varepsilon_{ci}} \sigma_{xi}\,d\varepsilon_{xi}}\right] \quad (12)$$

Ductility There are various type of ductility, which influence behavior. In this research strain ductility and displacement ductility were used to study the behavior of specimens. Therefore assuming linear strain distribution across the section under consideration and perfect bond between concrete and reinforcement the value of ductility in all post-yield states could be calculated. For this, curvature at any post-yield state (ϕ_p) is the ratio of concrete the compressive strain (ε_{cp}) at any post-yield state (p) to the depth of neutral axis (d_{np}) at corresponded state. On the other hand, curvature at the yield state (ϕ_y) is the ratio of ε_{sy} to the ($d-d_{np}$). Hence the ductility obtained is given by equation 13.

$$\mu_p = \frac{\phi_p}{\phi} = \frac{\varepsilon_{ci}\,(d-d_{np})}{\varepsilon_{sy}\,d_{np}} \quad (13)$$

Theoretical evaluation of the displacement ductility for all specimens was carried out at any post-yield state of behavior. It was assumed that Δ_y at the top of the column corresponded to the first yield of the section. In this research the displacement at ultimate state Δ_u corresponded to the ultimate load. The prediction of ultimate curvature ϕ_u was carried out using the ACI method and the values based on test results. Assuming that the strain of the first yield of reinforcement in the tension side of the column section, and concrete compressive strain at extreme fiber equal to 0.003, the ductility of the section, according to the method described by ACI 318, can be evaluated by:

$$\mu_\phi = \frac{\phi_u}{\phi_y} = \frac{\beta_1 d\varepsilon_{cu}\,(1-k)}{\alpha\varepsilon_{sy}} \quad (14)$$

In equation (14) the value of β_1 shall be taken as 0.85 for concrete strengths up to and including 30MPa. For concrete strengths above 30MPa, β_1 30MPa, shall be reduced continuously at a rate of 0.008 for each 1MPa of strength in excess of 30MPa. However, β_1 shall not be assumed to be less than 0.66. The values of k and a are given respectively as:

$$k = \left[(\rho+\rho')^2 m^2 + \left(\rho+\rho'\frac{d'}{d}\right)m\right]^{1/2} - (\rho+\rho')\,m \quad (15)$$

$$\alpha = \frac{A_s f_y - A_s f'_s}{0.85\,b f'_c} \quad (16)$$

In these equations ε_{cu} and ε_{sy} are the concrete compressive strain at ultimate state and the yield strain of reinforcement. The modular ratio is represented by m and b is the width of the wall, ρ and ρ' are the tensile and compressive steel percentage respectively. Compression and tension forces of longitudinal steel at yield state are represented by As fy and A'_s f'_y respectively.

RESULTS AND DISCUSSION

A summary of the test results for all specimens is presented in Table 3. Column performance was evaluated with respect to the moment capacity, displacement ductility and curvature ductility attained, the overall hysteresis behavior, and energy dissipation characteristics.

Hysteresis behavior Typical load-displacement hysteresis curves for tests on all specimens are shown Figure 9. The hysteresis curves for all specimens show fairly good stability but near the ultimate state of behavior ie, at last two cycles a drop in load-carrying capacity was observed, and

the connection exhibited good strength rather than energy absorption. Comparing the curves shown in Figure 9 the hysteresis behavior observed in the group 1 and 2 specimens appear quite similar. The load carrying capacity of cgroup-1 specimens is approximately 17 percent more than the specimens of group-2. The hysteresis curves contains sharp reductions in slope after the yield state which implies that the rate of bond deterioration in the connection region is high compared to elastic state of behavior.

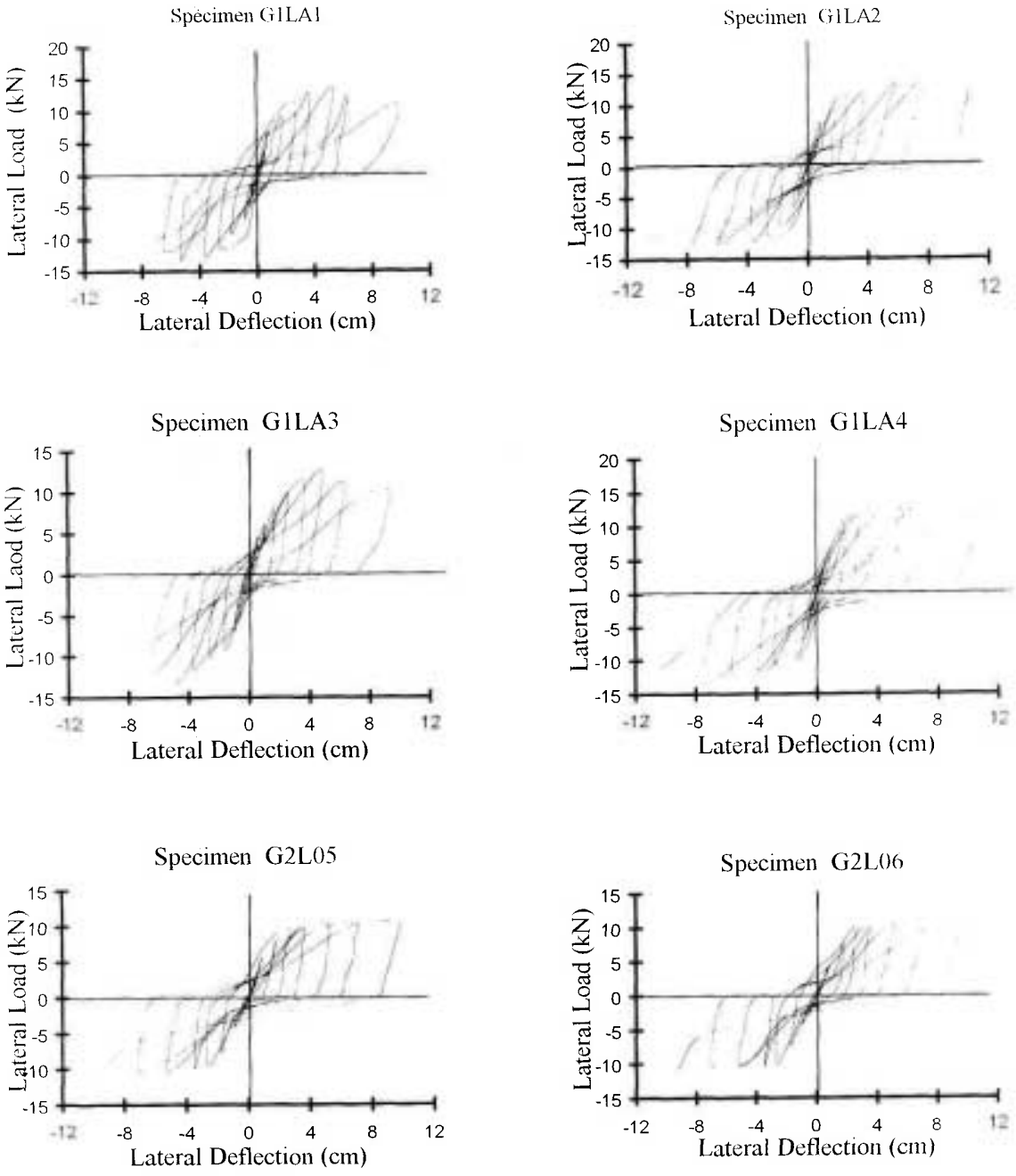

Figure 9. Lateral load vs lateral displacement for all specimens.

TABLE 3. Experimental and Theoretical Ultimate Moments, All Specimens

Specimen	Load Direction →			Load Direction ←		
	Experiment Kn-m (1)	Theory Kn-m (2)	(2)/(1)	Experiment Kn-m (3)	Theory Kn-m (4)	(4)/(3)
G1LA1	9.1775	7.4197	0.76	8.8485	7.0504	0.80
G1LA2	9.1510	8.2215	0.90	8.5073	7.0553	0.83
G1LA3	8.5420	7.0203	0.82	8.8956	7.0549	0.79
G1LA4	8.3411	7.0641	0.85	8.0220	7.0606	0.88
G2LO5	7.3780	6.9034	0.94	7.5460	6.8837	0.91
G2LO6	7.6580	6.8928	0.90	7.6300	6.9203	0.91

Energy Dissipation The energy dissipated by a column during a particular load cycle can be represented by the area enclose by the force-displacement hysteresis curve. the energy dissipated by an idealized perfectly elasto-plastic system during a complete displacement cycle is the area surrounded by parallelogram (ABCD), as shown in Figure 10. For a particular displacement ductility factor, $\mu_\Delta = \Delta_u/\Delta_y$, the idea plastic energy dissipated can be computer as:

$$E_p = 4\left[\Delta_u - \Delta_y\right] F_p$$

or

$$E_p = 4\left[\mu_\Delta - 1\right] \Delta_y F_p \qquad (18)$$

Where F_p is the maximum force corresponding to the displacement level [8]. To evaluate quantitatively the energy dissipation capacity of the different specimens, the actual energy dissipation E_i at any one cycle of loading corresponding to post-yielding state was divided by the E_p value for the same displacement ductility factor. Plots of E_i/Ep values versus displacement ductility factor μ_Δ for all specimens are shown in Figure 11. As the Figure shows, the observed energy dissipation effectiveness for group 1 specimens is almost similar. At low displacement ductility factor the responses of group 1 are greater than those of group-2. however, at large displacement ductility factor, the energy dissipation for both groups is approximately similar.

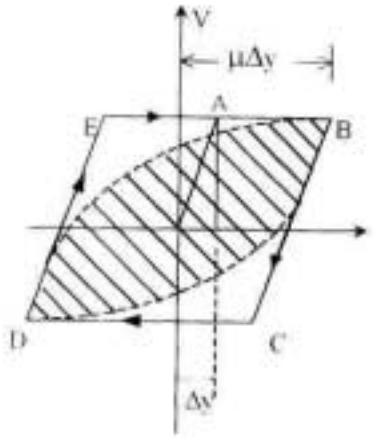

Figure 10. Actual and idealized perfectly elasto-plastic hysteresis curves.

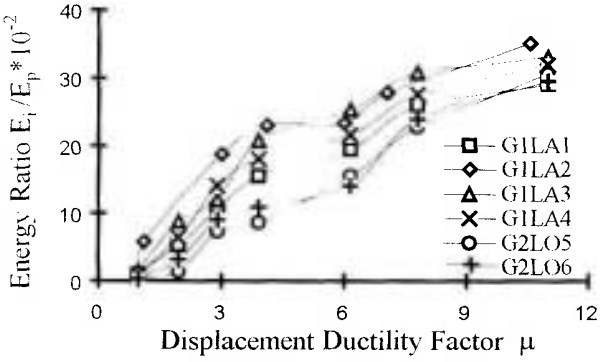

Figure 11. Energy dissipation curves for all specimens.

Cracking Patterns and behavior It must be emphasized that all specimens failed mainly in flexure. The first flexural cracks in the first group specimens developed at critical section and propagated in successive cycle on two column faces perpendicular to the plane of lateral load. Diagonal cracks developed on column faces parallelled to lateral load direction and there was a considerable increase in their width and length as the load was increased. Specimen G1LA1 and G1LA3 exhibited concrete crush after cycle seven ($\mu_\Delta = 6$) and that G1LA2 and G1LA4 after cycle number eight ($\mu_\Delta = 8$). At these stages longitudinal bars of column buckled. The results are in good agreement with the criteria given in reference 6. Another important observation that the concrete grouts was neither cracked nor crushed even at failure. On the other hand, the column come out from the pocket of the footing during the last cycles when the plastic behavior was observed. This phenomenon indicates that this kind of connection is not fully fixed and causes considerable reduction in strength and energy dissipation. Group 2 specimens exhibit rapid development of flexural cracks at critical section and along the column height. In this case too shearing cracks developed similar to those 7 the first group. As indicated before the failure of these specimens was due to flexure. Flexural cracks propagate and cover the whole face of the column. Buckling of column's main bars and crushing of concrete occurred at last cycle. The columns came out more from the pocket of footing compared to those in first group specimens. The absence of axial load in this group makes the comparison between two groups easy. Ogawa and Shiga [6] who worked on monolithic column footing connection indicated that increase in axial load causes rapid crushing of concrete in compression. Comparsion between the two groups of specimens indicates the same result. The strength of the first group is more than that of the second group. The ratio of theoretical moment to that of experimental is given in Table 3 which shows good agreement.

Ductility Ductility defines the deformational capacity of structural members limited with minimum reduction in strength. Table 4 gives the value of ductility for all specimens based on Δ_u/Δ_y and ϕ_u/ϕ_y rations. The measured displacement at yield state was controlled through electrical strain gauges, i.e. when the strain of main bars of column reached the value of 0.2% the load and displacement reading were recorded.

Alos curvature at ultimate state was calculated based on ACI method as well as the method using mathematical model [5]. Then ductility based on ϕ_u/ϕ_y was evaluated.

The values of ductility in Table 4 indicate that all specimens exhibited excellent ductile behavior. Although the curvature ductility is approximately the same for all 6 specimens, the displacement ductility for specimens of group-2 is relatively high. The reason behind that is the absence of axial load for this group. On the other hand the axial load prevent the large displacement at the top of the specimens, while it has little effect on the base of the column where curvature ductility was evaluated for this section. Figure 9 shows the lateral load displacement characteristics of all specimens tested. They also indicate good ductile behavior and reduction in strength, which was mainly due to sliding of the columns.

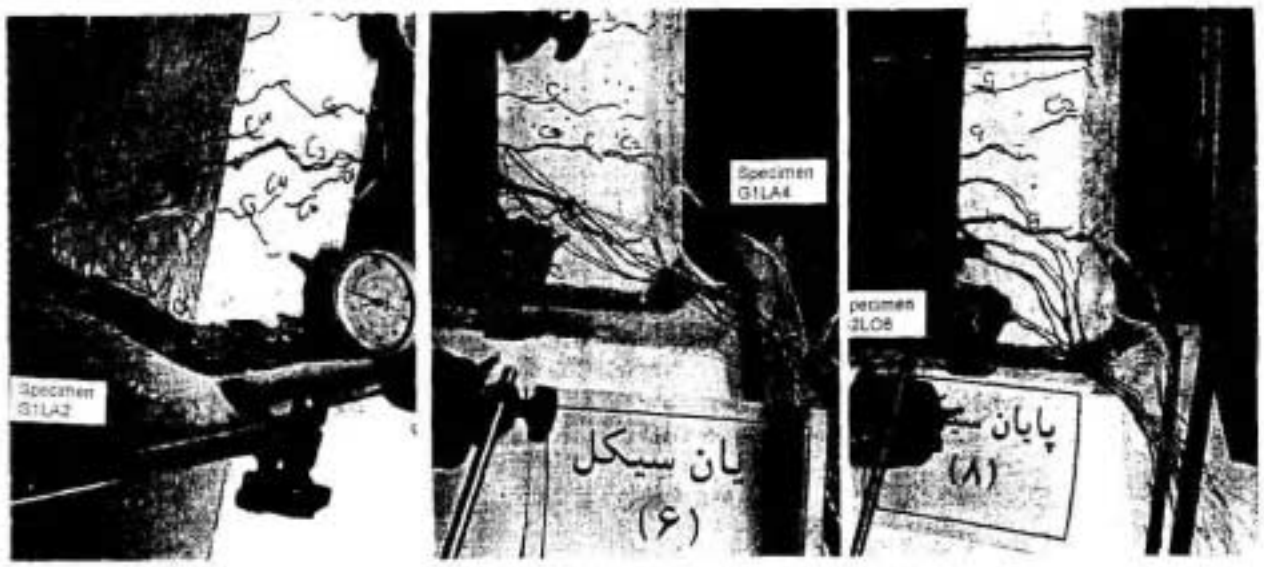

Figure 12. Failure mode of specimens G1LA2, G1LA4 and G2LO6.

TABLE 4. Curvature and Displacement Ductility on the Basis of fu/fu and Du/Dy.

				Ductility based on ϕ_u/ϕ_u		Ductility based on Δ_u/Δ_y		
Sspecimen	(1) ϕ_y*10^{-4} **Yield State**	(2) ϕ_u*10^{-4} **ACI Method**	(3) ϕ_u*10^{-4} **Mathe Method**	$\mu_\phi = \frac{(2)}{(1)}$	$\mu_\phi = \frac{(3)}{(1)}$	Δ_y (mm)	Δ_u (mm)	$\mu_\phi = \Delta_u/\Delta_y$
G1LA1	2.502	12.52	13.04	5.00	5.21	9.0	55.0	6.11
G1LA2	2.930	12.52	13.04	4.27	4.45	9.5	75.5	7.95
G1LA3	3.000	12.52	13.04	4.17	4.35	8.8	53.2	6.05
G1LA4	2.815	12.52	13.04	4.45	4.64	9.4	75.0	7.98
G2LO5	2.482	14.51	14.95	5.85	6.02	8.7	96.0	11.0
G2LO6	2.407	14.51	14.95	6.03	6.21	8.5	94.0	11.0

CONCLUSIONS

The following conclusions are draw based on the results and observations presented in this paper.

1. The specimens representing prefabricated connections exhibited rapid degradation in stiffness and strength once the capacity of the connection reached. This was attributed on the flexural failure of the joint.
2. The failure of the specimens occurred at tension side and due to the presence of axial load on group-1 unit tests their ultimate flexural strength was greater than that group-2 specimens.
3. Crack patterns in group-2 specimens formed at early stages but the crushing of concrete in compression zone occured later than

group-1 specimens.

4. The detail and connection used in this study proved successful in flexural strength rather than the curvature ductility. Sliding of column from the footing pocket causes reduction in ductility.
5. The deformational responses of the specimens were found to be inadequate due to sliding of the column from the footing pocket. This caused considerable reduction in stiffness and energy dissipation of the specimens.

ACKNOWLEDGEMENT

The author gratefully acknowledges the financial support of BHRC of Islamic Republic of Iran. The research formed as MSc. dissertation for Mr. M. R. Hamidian carried out in the structural laboratory of BHRC, which itself is a part of a project entitled as "Experimental Study of Typical Iranian Reinforced Concrete Urban Construction" under the supervision of the author.

QUOTATION

E_i = Dissipated energy at any one cycle of loading
E_p = Dissipated energy in idealized perfectly elasto-plastic state.
E_p = Lateral load applied to the column
F_c = Concrete cylinder strength at 28 days
F_{ct} = Concrete splitting tensile strength at 28 days
Δ_y = Displacement corresponding to yield state
Δ_u = Displacement corresponding to ultimate state
ϕ_y = Curvature at yield state
ϕ_u = Curvature at ultimate state
μ_Δ = Displacement ductility factor = Δ_u/Δ_y
M_ϕ = Curvature ductility factor = ϕ_u/ϕ_y

REFERENCES

1. Iranian Code for Minimum Applied Load to the Buildings, IS-519, (1960).
2. Iranian Code for Seismic Resistant Design of Buildings, IS-2800, (1988).
3. Building Code Requirements for Reinforced Concrete, ACI-318M-89, (1989).
4. Neville, A. M. and Brooks, J.J. "Concrete Technology". Longman, London, (1987).
5. Tasnimi, A. A, "Prediction of Forces Within Prestressed Sections", Ph.D Thesis, Dept. of Civil and Structural Engineering University of Bradford, UK (1988).
6. Junji O. and Toshio S., "Earthquake Damage Index for Reinforced Concrete Columns", ***Proceeding of the Ninth World Conference on Earthquake Engineering***, Japan, (Aug. 2-9, 1988) Vol.4, 425.
7. Tasnimi, A. A, and Mossayebi, A. "Cyclic behavior of Exterior Beam-Column Joints in Precast Concrete Frames", ***3rd International KERENSKY Conference on Structural Engineering***, Singapore, (20-22 July 1994).
8. Ang, B. G, Priestly, M. J. N and Paulay, T., "Seismic Shear Strength of Circular Bridge Piers", Research Report 85-5, Department of Civil Engineering, University of Canterbury, Christchurch New Zeland, July, (1985), 480p.
9. Gajanan M., Sabnis, H. G. H. and Other, "Structural Modeling and Experimental Techniques", Prentice-Hall, Inc, England Cliffs, (1983).